Week 9
Lecture Notes:
Topological Condensed Matter Physics

Sebastian Huber and Titus Neupert

Department of Physics, ETH Zürich
Department of Physics, University of Zürich

Chapter 9

Topological Crystalline Insulators II: Topological quantum chemistry

Learning goals

- We understand what we mean by Wannierizablity.
- We know how to think of a band as a representation of the space group.
- We know how to construct elementary band representations.
- We can use the Bilbao server to analyze bands according to their symmetry properties.

- B. Bradlyn, L. and Elcoro, J. Cano, M. G. Vergniory, Z. Wang, C. Felser, M. I. Aroyo, and B. A. Bernevig, Nature **537**, 298 (2017)

9.0 Prerequisites

In this chapter we introduce a way to characterize the topology of Bloch bands stabilized by space group symmetries. To this end we will construct representations of the infinite space groups (the group of discrete translations are not closed under a finite number of group elements). As a prerequisite we build on basic knowledge of representation theory. In particular, we assume that you know

1. what an irreducible representation (irrep) is.
2. that irreps of dimension larger than one may split, if the symmetry is reduced. For example the p_x, p_y, p_z orbitals forming the spin-1 triplet

$$+ : p_x + \mathrm{i}p_y \tag{9.0.1}$$
$$0 : p_z \tag{9.0.2}$$
$$- : p_x - \mathrm{i}p_y \tag{9.0.3}$$

   are splitting into the two individual irreps of $p_x \pm \mathrm{i}p_y$ and p_z if $SO(3)$ is reduced to, e.g, C_{4v}.
3. how to use character tables to do this symmetry reduction.
4. about double groups: If spin-1/2 particles are involved, we supplement all group elements to also appear with an additional rotation by 2π. For the irreps where a spin-1/2 particles is involved all characters acquire a minus sign by this. Their names typically carry a bar as for example in $\overline{E}_{1g}$.

9.1 Wannierizability

In a band insulator we are free to choose a basis in which to write down the wave-functions of all filled bands. Let us consider a Bloch problem

$$\sum_{\beta} \mathcal{H}_{\alpha,\beta}(\boldsymbol{k}) u_{\boldsymbol{k};a,\beta} = \epsilon_a(\boldsymbol{k}) u_{\boldsymbol{k};a,\alpha} \tag{9.1.1}$$

where a enumerates the energy bands, $\boldsymbol{k}$ runs over the Brillouin zone and α, β encode some orbital or sub-lattice degree of freedom. We can go from a momentum space picture to a real space description in term of *Wannier functions*

$$\psi_{a,\alpha}(\boldsymbol{r} - \boldsymbol{R}_i) = \int_{\mathrm{BZ}} \mathrm{d}^d \boldsymbol{k}\, u_{\boldsymbol{k};a,\alpha} e^{\mathrm{i}\boldsymbol{k}\cdot(\boldsymbol{r}-\boldsymbol{R}_i)}. \tag{9.1.2}$$

If we want these Wannier functions to serve as a basis for the ground-state, we have to consider all $a \leq n$, where n is the number of filled bands. Already in 1959 Walter Kohn [3] realized, that the Wannier functions are only exponentially decaying if we choose Bloch functions $u_{\boldsymbol{k};a,\alpha}$ which are smooth in $\boldsymbol{k}$.[1] Given what we learned in the last chapters, we immediately observe that $\psi_{a,\alpha}(\boldsymbol{r} - \boldsymbol{R}_i)$ are gauge dependent under a set of $\mathrm{U}(n)$ transformations (one per $\boldsymbol{k}$). In other words, we need to choose a *smooth* $\mathrm{U}(n)$ *gauge* for the Wannier functions to be exponentially localized. We know, however, that the topological indices introduced in Chap. 7 are only non-vanishing if there is an obstruction to choose a smooth gauge.[2] *Therefore, we can also use the (in-) ability to choose a set of basis functions which are all exponentially localized as a definition for a topological system:* If we can smoothly transform the $\psi_{a,\alpha}(\boldsymbol{r} - \boldsymbol{R}_i)$ to be exponentially localized, i.e., if we can choose an *atomic limit*, we call a system *trivial*. Finally, we have seen that symmetries can give rise to topological phases that would be trivial in their absence, i.e., the adiabatic path to the atomic limit may now be obstructed by the constraints imposed by the symmetry. The same holds here: We demand the atomic limit to be compatible with a set of (crystalline) symmetries.

We are now in the position to define *Wannierizablity*. We call a set of bands Wannierizable if we can find a basis transformation to a set of wave-functions $\psi_{a,\alpha}(\boldsymbol{r} - \boldsymbol{R}_i)$ that are symmetric and exponentially localized. If a set of bands is not Wannierizable, we call it topological.

An important remark is in order: If we formulate a tight-binding model for a set of bands, we implicitly assume that we used exponentially localized wave-functions when we wrote down the Hamiltonian. Therefore, the set of all bands together arising from such a tight-binding model are bound to be trivial. The only option to have topological phases is, if there is more than one band and they are separated by a gap.

With these introductory remarks, we can outline the program of what goes under the name of *topological quantum chemistry* [1]. The symmetries we are dealing with are the 230 space groups, i.e., all symmetry groups arising in crystalline systems. The core idea is, that we can *construct all possible band-structures that can arise from symmetric Wannier functions* positioned in a lattice obeying one of the 230 symmetry groups. Once one achieves this goal, one has, by construction, an *exhaustive list of all trivial bands in each of the space groups*. Using this exhaustive list, we can check for any band-structure we obtain for a concrete problem if and how it fits into this exhaustive table. If it does not, we know we deal with a topological band. As an additional bonus we will see how this approach gives rise to two main classes of topological bands: stable topological and fragile topological. While the latter sounds like an oxymoron, we will see that this type of topology is neither "weak" nor esoteric.

[1] Remember that that the Fourier transformation of a function $u_{\boldsymbol{k}}$ that is s-fold differentiable is falling off at least as $1/|\boldsymbol{x}|^s$. Hence, only for C^∞-functions can we expect exponentially localized Wannier functions.

[2] Remember that the Berry curvature $\boldsymbol{\mathcal{F}}$ can be written as the (higher-dimensional generalizations) curl of a vector field $\boldsymbol{\mathcal{A}}$. Hence, by using Stoke's theorem on a closed manifold (the d-torus) we obtain a zero index if the Berry connection $\boldsymbol{\mathcal{A}}$ is free of divergencies.

In the following, we will introduce all the needed definitions and develop the general strategy. We illustrate all these developments on the example the doubled lattice Dirac model introduced in Chap. 4.

9.2 Space groups

Theory: To introduce space groups we need to fix a few facts about crystals. Crystals are built from Bravais lattices where every *unit cell* in the lattice can be reached by a *discrete translation*

$$\boldsymbol{t} = n_i \, \boldsymbol{a}_i \qquad \text{with} \qquad \boldsymbol{n} \in \mathbb{Z}^d, \tag{9.2.1}$$

where the $\boldsymbol{a}_i$ are the lattice vectors. The Bravais lattice is isomorphic to $\mathbb{Z}^d$ and the group of translations $\{\boldsymbol{t}\}$ on the Bravais lattice is an *infinite group*. Note, that inside the unit cell, atoms can be arranged in arbitrary positions, called Wyckoff positions. The full symmetry group of the crystal can now be written as all operations that leave the crystal invariant and is called a space group G with elements g written as

$$g = \{R|\boldsymbol{r}\}. \tag{9.2.2}$$

The elements of R are in the *crystallographic point group* which leave one point invariant[3] and $\boldsymbol{r}$ are translations. The action of a group element g on a point in space $\boldsymbol{q}$ is given by

$$g\boldsymbol{q} = R\boldsymbol{q} + \boldsymbol{r}. \tag{9.2.3}$$

Note, that the space group generically contains pure translations $\{\mathbb{1}|\mathbf{t}\}$, pure point group operations $\{R|0\}$, as well as non-symmorphic elements which involve, e.g, a mirror operation and a half-lattice translation.
As we intend to investigate what kind of bands can be induced by symmetric orbitals, we need to talk about where we put these orbitals and what it means to be symmetric at the chosen locations. A generic point $\boldsymbol{q}$ inside the unit cell is called a *Wyckoff position*. For the remainder of this chapter we need the "most symmetric" positions called *maximal Wyckoff positions*.[4] Note that a Wyckoff position might not be invariant under all point group operations. The non-trivial images $g\boldsymbol{q} = R^{-1}\boldsymbol{q}$ form the *orbit* of such a position.
Example: We are interested in a system in the space group No. 123, also called $P4/mmm$. In fact, for the purpose of this lecture we are only interested in the planar version of $P4/mmm$. However, we need the out-of plane point group elements to fix the orbitals that we put onto the two-dimensional lattice.
The two dimensional Bravais lattice is generated by the lattice vectors

$$\boldsymbol{a}_1 = (1, 0), \tag{9.2.4}$$
$$\boldsymbol{a}_2 = (0, 1). \tag{9.2.5}$$

The space group $P4/mmm$ does not contain any non-symmorphic elements, i.e, all space group elements can be written as either $\{\mathbb{1}|\boldsymbol{t}\}$ with $\boldsymbol{t} = n_i\boldsymbol{a}_i$ or $\{R|0\}$ with $R \in D_{4h}$, the dihedral point group of $P4/mmm$.
In Fig.9.1, we show the unit cell, the maximal Wyckoff positions, and the action of all generators of the group D_{4h}. Note that the maximal Wyckoff positions $1a$ and $1b$ have the full D_{4h} point group as their site-symmetry. At $2c$, the symmetry is reduced to D_{2h}.

[3] A point group is a symmetry group that leaves a point invariant. A *crystallographic* point group is a point group that is compatible with one of the Bravais lattices. As such, they can only contain discrete rotations, in fact rotations of order 1, 2, 3, 4, and 6. There are only 32 crystallographic point groups.

[4] We can define the *stabilizer group* $G_{\boldsymbol{q}}$, a subgroup of the full group G which leaves the point $\boldsymbol{q}$ invariant. The

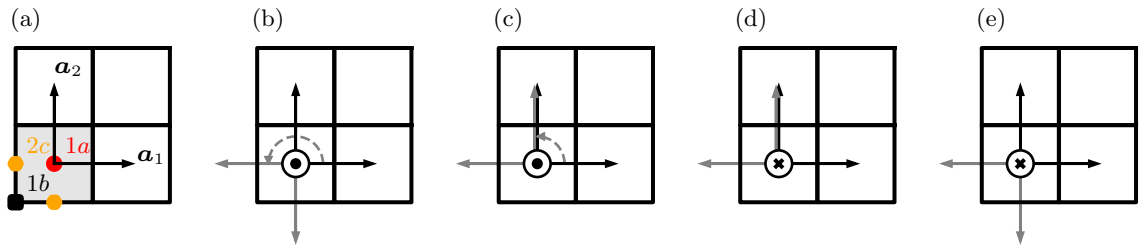

Figure 9.1: The space group $P4/mmm$: (a) The lattice vectors $\boldsymbol{a}_{1/2}$, the unit cell, and the maximal Wyckoff positions $1a$, $1b$, $2c$. (b) The action of the two-fold rotation around the z-axis C_2^z, or in Schönflies notation 2_{001}. (c) The action of a fourfold rotation around the z-axis C_4^z, or in Schönflies notation 4^+_{001}. (d) The action of the two-fold rotation around the y-axis C_2^y, or in Schönflies notation 2_{010}. Note, that for the in-plane drawing, this is identical to a mirror on the y-axis $M_x = I \circ C_2^z \circ C_2^y$, or in Schönflies notation m_{100}. (e) The action of inversion I, or in Schönflies notation -1.

9.2.1 Placing orbitals

Theory: The next step in our program is to place atoms, or more precisely, orbitals at maximal Wyckoff positions.[5] Once we put these orbitals, they will hybridize and form the sought after Bloch bands.

Free atoms are typically symmetric under the action of $SO(3)$. When we place these into the lattice, the symmetry is reduced to the one of the respective Wyckoff positions. This is an example of subduction: The irreducible representations of a larger group (here $SO(3)$) give rise to representations of a smaller group.

Example: Let us put spinful orbitals at the Wyckoff position $1a$. At $1a$ we have the full symmetry D_{4h}, hence we have to consider the double group D_{4h}. A minimal set of characters is given in Tab. 9.1. The Bilbao Crystallographic Server provides most information.

D_{4h}

		$\mathbb{1}$	C_4^z	I	$\bar{C}_4^z$
$\overline{E}_{2g}$	$\overline{GM}_6$	2	$-\sqrt{2}$	2	$-\sqrt{2}$
$\overline{E}_{1g}$	$\overline{GM}_7$	2	$\sqrt{2}$	2	$\sqrt{2}$
$\overline{E}_{2u}$	$\overline{GM}_8$	2	$-\sqrt{2}$	-2	$\sqrt{2}$
$\overline{E}_{1u}$	$\overline{GM}_9$	2	$\sqrt{2}$	-2	$-\sqrt{2}$

D_{2h}

		$\mathbb{1}$	I
$\overline{E}_g$	$\overline{GM}_5$	2	2
$\overline{E}_u$	$\overline{GM}_6$	2	-2

C_s

		$\mathbb{1}$	M_{01}
${}^2\overline{E}$	$\overline{GM}_3$	1	$-\mathrm{i}$
${}^1\overline{E}$	$\overline{GM}_4$	1	i

Table 9.1: Reduced set of characters of the spin-1/2 irreducible representation of the double group D_{4h} and some if its subgroups. The first two columns in each table indicate standard names of the irreps, the following columns contain the characters of the conjugacy classes that we need here. Note that $\bar{C}_4^z = I \circ C_4^z$ is an improper rotation. All other characters not shown are either zero or related by a minus sign due to the addition of a 2π rotation. The generators of all groups can be found on the Bilbao Crystallographic Server for D_{4h}, D_{42h}, C_s, and likewise for the full character tables D_{4h}, D_{2h}, C_s.

Let us start from the following $SO(3)$ irrep: Out of an s-wave orbital ($L = 0$) and a spin=1/2

orbit of a Wyckoff position $\boldsymbol{q}$ is the set of all points generated from $\boldsymbol{q}$ by the application of all $g \in G$ onto that point. This leads to the *multiplicity of a Wyckoff postion*: the number of points in the orbit of $\boldsymbol{q}$. Finally, we can define *maximal Wyckoff positions*: a Wyckoff position $\boldsymbol{q}$ is non-maximal if there exists a group H such that $G_{\boldsymbol{q}} \in H \in G$. A Wyckoff position that is not non-maximal is maximal. Examples for maximal Wyckoff positions are those, where $G_{\boldsymbol{q}}$ contains a non-trivial rotation.

[5] One can of course place atoms at arbitrary Wyckoff positions. However, for the sake of the topological classification of the Bloch bands, the maximal Wyckoff positions suffice [2].

($S = 1/2$) we form the representation with $J = L + S = 1/2$ spanned by $|s,\uparrow\rangle$ and $|s,\downarrow\rangle$. Remember that the representation of a rotation for a general angular momentum state J are given by

$$\rho(\mathbf{\Omega}) = e^{\mathrm{i}\boldsymbol{J}\cdot\mathbf{\Omega}}, \tag{9.2.6}$$

where $\boldsymbol{J}$ denote the angular momentum matrices $\boldsymbol{J} = (J_x, J_y, J_z)$, $\Omega = |\mathbf{\Omega}|$ is the rotation angle and $\hat{\mathbf{\Omega}} = \mathbf{\Omega}/\Omega$ the rotation axis. When using the Pauli matrices $J_i = \frac{1}{2}\sigma_i$ for $J = 1/2$ we obtain

$$\begin{aligned}
\rho(C_2^z) &= \begin{pmatrix} \mathrm{i} & 0 \\ 0 & -\mathrm{i} \end{pmatrix} && \operatorname{tr}\rho(C_2^z) = 0, \\
\rho(C_4^z) &= \begin{pmatrix} e^{\mathrm{i}\pi/4} & 0 \\ 0 & e^{-\mathrm{i}\pi/4} \end{pmatrix} && \operatorname{tr}\rho(C_4^z) = \sqrt{2}, \\
\rho(C_2^y) &= \begin{pmatrix} 0 & 1 \\ -1 & 0 \end{pmatrix} && \operatorname{tr}\rho(C_2^y) = 0, \\
\rho(I) &= \begin{pmatrix} 1 & 0 \\ 0 & 1 \end{pmatrix} && \operatorname{tr}\rho(I) = 2.
\end{aligned} \tag{9.2.7}$$

The last line we extract from the fact that s-orbitals are even under inversion. When comparing the characters with those in Tab. 9.1 we immediately see that we deal with $\overline{E}_{1g}$.
As a second example, let us consider p-orbitals ($L = 1$) and a spin=1/2 ($S = 1/2$). This time, we want to consider $J = L + S = 3/2$. Using the rotation matrices for $J = 3/2$ we obtain

$$\begin{aligned}
\rho(C_2^z) &= \begin{pmatrix} -\mathrm{i} & 0 & 0 & 0 \\ 0 & \mathrm{i} & 0 & 0 \\ 0 & 0 & -\mathrm{i} & 0 \\ 0 & 0 & 0 & \mathrm{i} \end{pmatrix} && \operatorname{tr}\rho(C_2^z) = 0, \\
\rho(C_4^z) &= \begin{pmatrix} e^{3\mathrm{i}\pi/4} & 0 & 0 & 0 \\ 0 & e^{\mathrm{i}\pi/4} & 0 & 0 \\ 0 & 0 & e^{-\mathrm{i}\pi/4} & 0 \\ 0 & 0 & 0 & e^{-3\mathrm{i}\pi/4} \end{pmatrix} && \operatorname{tr}\rho(C_4^z) = 0, \\
\rho(C_2^y) &= \begin{pmatrix} 0 & 0 & 0 & 1 \\ 0 & 0 & -1 & 0 \\ 0 & 1 & 0 & 0 \\ -1 & 0 & 0 & 0 \end{pmatrix} && \operatorname{tr}\rho(C_2^y) = 0, \\
\rho(I) &= \begin{pmatrix} -1 & 0 & 0 & 0 \\ 0 & -1 & 0 & 0 \\ 0 & 0 & -1 & 0 \\ 0 & 0 & 0 & -1 \end{pmatrix} && \operatorname{tr}\rho(I) = -4.
\end{aligned} \tag{9.2.8}$$

Again, the inversion matrix we obtain from the fact that p-orbitals are odd under inversion. We see that by going from $SO(3) \to D_{4h}$ we can further reduce the $J = 3/2$ representation as the states with $m_J = \pm 3/2$ are not mixing with $m_J = \pm 1/2$. We choose the $m_J = \pm 3/2$ sector

spanned by $|p_x + \mathrm{i}p_y, \uparrow\rangle$ and $|p_x - \mathrm{i}p_y, \downarrow\rangle$. The representations are given by

$$\begin{aligned}
\rho(C_2^z) &= \begin{pmatrix} -\mathrm{i} & 0 \\ 0 & \mathrm{i} \end{pmatrix} && \operatorname{tr}\rho(C_2^z) = 0, \\
\rho(C_4^z) &= \begin{pmatrix} e^{3\mathrm{i}\pi/4} & 0 \\ 0 & e^{-3\mathrm{i}\pi/4} \end{pmatrix} && \operatorname{tr}\rho(C_4^z) = -\sqrt{2}, \\
\rho(C_2^y) &= \begin{pmatrix} 0 & -1 \\ 1 & 0 \end{pmatrix} && \operatorname{tr}\rho(C_2^y) = 0, \\
\rho(I) &= \begin{pmatrix} -1 & 0 \\ 0 & -1 \end{pmatrix} && \operatorname{tr}\rho(I) = -2.
\end{aligned} \tag{9.2.9}$$

Consulting Tab. 9.1, we see that we work with $\overline{E}_{2u}$. In the following, we want to place these two irreps at $1a$ and investigate what bands can arise from these orbitals.

9.2.2 Inducing a representation of the full space group

Theory: Now that we know which orbitals we place at the maximal Wyckoff positions, we can see how the resulting Bloch wave functions transform under the space group symmetries. To this end, we first take the Fourier transformation back to Bloch states

$$u_{i,\alpha}(\boldsymbol{k}, \boldsymbol{r}) = \frac{1}{\sqrt{N}} \sum_{\mu} e^{\mathrm{i}\boldsymbol{k}\cdot\boldsymbol{t}_\mu} \psi_{i\alpha}(\boldsymbol{r} - \boldsymbol{t}_\mu). \tag{9.2.10}$$

Here, the $\boldsymbol{t}_\mu$ denote the lattice vectors. Note, that opposed to in (9.1.2), we label the orbitals i and the Wyckoff position α individually. We also made the number of unit cells N explicit. Moreover, we do not specify a Hamiltonian yet, so we cannot provide a band label a. All we want to investigate is, how the Bloch states transform under the space group symmetries. As we construct the Bloch states from Wannier states in specific irreps of the point group, we can now deduce how the Bloch states transform. In other words, our procedure of placing well defined irreps at all sites of the crystal and then taking a Fourier transform allows us to *induce a representation* of the (infinte) space group from the irreps of the (finite) point group.
Let us quickly see how we know the transformation of a Wannier state $\psi_{i\alpha}(\boldsymbol{r} - \boldsymbol{t}_\mu)$ under the point group symmetries. For this, we need to know how each orbital transforms around its Wyckoff position. Once we fix this, we will see how they transform in the full lattice.
For the transformation around a single site we reduce all our consideration to the transformation properties of one representative Wyckoff position $\alpha = 1$ in the orbit:

$$g\psi_{i1} = [\rho(g)]_{ji}\psi_{j1}. \tag{9.2.11}$$

For any other Wyckoff position $\boldsymbol{q}_\alpha$ in the orbit of $\boldsymbol{q}_1$ we first bring the Wannier function to position $\alpha = 1$ by the use of

$$\psi_{i\alpha}(\boldsymbol{r}) = g_\alpha\psi_{i1}(\boldsymbol{r}) = \psi_{i1}(g_\alpha^{-1}\boldsymbol{r}) \tag{9.2.12}$$

We then inherit the representation of h at α from the reference position 1

$$h\psi_{i\alpha} = \underbrace{g_\alpha g g_\alpha^{-1}}_{h} g_\alpha\psi_{i1} = g_\alpha g\psi_{i1} = g_\alpha[\rho(g)]_{ji}\psi_{j1} = [\rho(g_\alpha^{-1}hg_\alpha)]_{ji}\psi_{j\alpha}. \tag{9.2.13}$$

This formula is easy to understand. Imagine you consider the Wyckoff $2c$ in $P4/mmm$ which has two points in the orbit: $\alpha = 1:\ (1/2, 0)$ and $\alpha = 2:\ (0, 1/2)$. $2c$ has the site symmetry group D_{2h}. The mirror $h = m_{01}$ at $\alpha = 1$ corresponds to the the mirror $g = m_{10}$ at $\alpha = 2$. The factor $g_\alpha^{-1}hg_\alpha$ is reflecting just that with $g_\alpha = C_4^z$.

Now that we know the local transformation, let us move to the question how the orbitals in the full lattice transform. It is this step, where we *induce a representation in the full space group G from the irreps of the point group:* $\rho_G = \rho \uparrow G$:

$$h\psi_{i\alpha}(\boldsymbol{r}-\boldsymbol{t}_\mu) = [\rho(g^h_{\alpha\beta})]_{ji}\psi_{j\beta}(\boldsymbol{r}-R\boldsymbol{t}_\mu-\boldsymbol{t}_{\alpha\beta}). \tag{9.2.14}$$

Let us analyze this formula step by step. First, under the action of h, the orbital might be transported into another unit cell

$$h\boldsymbol{q}_\alpha = \{\mathbb{1}|\boldsymbol{t}_{\alpha\beta}\}\boldsymbol{q}_\beta, \quad \text{with} \tag{9.2.15}$$

$$\boldsymbol{t}_{\alpha\beta} = h\boldsymbol{q}_\alpha - \boldsymbol{q}_\beta \tag{9.2.16}$$

We use (9.2.15) to obtain

$$\underbrace{g_\beta^{-1}\{\mathbb{1}|-\boldsymbol{t}_{\alpha\beta}\}hg_\alpha}_{g^h_{\alpha\beta}}\boldsymbol{q}_1 = \boldsymbol{q}_1, \tag{9.2.17}$$

which defines the group element g which leaves the Wyckoff position invariant and allows us to use the result (9.2.13) in (9.2.14).
With these results, we are in the position to determine how the Bloch functions transform

$$\begin{aligned}
[\rho_G(h)]_{j\beta,i\alpha}u_{j\beta}(\boldsymbol{k},\boldsymbol{r}) &= \frac{1}{\sqrt{N}}\sum_\mu e^{\mathrm{i}\boldsymbol{k}\cdot\boldsymbol{t}_\mu}[\rho_G(h)]_{j\beta,i\alpha}\psi_{j\beta}(\boldsymbol{r}-\boldsymbol{t}_\mu)\\
&\overset{(9.2.14)}{=} \frac{1}{\sqrt{N}}\sum_\mu e^{\mathrm{i}\boldsymbol{k}\cdot\boldsymbol{t}_\mu}[\rho(g^h_{\alpha\beta})]_{ji}\psi_{j\beta}(\boldsymbol{r}-R\boldsymbol{t}_\mu-\boldsymbol{t}_{\alpha\beta})\\
&= [\rho(g^h_{\alpha\beta})]_{ji}\frac{1}{\sqrt{N}}\sum_\mu e^{\mathrm{i}(R^{-1}\boldsymbol{k})\cdot(R\boldsymbol{t}_\mu)}\psi_{j\beta}(\boldsymbol{r}-R\boldsymbol{t}_\mu-\boldsymbol{t}_{\alpha\beta})\\
&= e^{-\mathrm{i}(R^{-1}\boldsymbol{k})\cdot\boldsymbol{t}_{\alpha\beta}}[\rho(g^h_{\alpha\beta})]_{ji}\frac{1}{\sqrt{N}}\sum_\mu e^{\mathrm{i}(R^{-1}\boldsymbol{k})\cdot(R\boldsymbol{t}_\mu+\boldsymbol{t}_{\alpha\beta})}\psi_{j\beta}(\boldsymbol{r}-R\boldsymbol{t}_\mu-\boldsymbol{t}_{\alpha\beta})\\
&= e^{-\mathrm{i}(R^{-1}\boldsymbol{k})\cdot\boldsymbol{t}_{\alpha\beta}}[\rho(g^h_{\alpha\beta})]_{ji}u_{j\beta}(R^{-1}\boldsymbol{k},\boldsymbol{r}).
\end{aligned}$$

With this we achieved our goal! We have found a representation of the space group G of the form

$$[\rho^{\boldsymbol{k}}_G(h)]_{j\beta,i\alpha} = e^{-\mathrm{i}(R^{-1}\boldsymbol{k})\cdot\boldsymbol{t}_{\alpha\beta}}[\rho(g^h_{\alpha\beta})]_{ji}. \tag{9.2.18}$$

It is quadratic matrix of size $n_{\text{orbit}}d_{\text{orbitals}} \times n_{\text{orbit}}d_{\text{orbitals}}$ where n_{orbit} is the number of Wykoff positions in the orbit and d_{irrep} is the dimension of the irrep we place on these maximal Wyckoff positions. In $\boldsymbol{k}$-space it connects a pair of two momenta $\boldsymbol{k}$ and $R^{-1}\boldsymbol{k}$. We close this section by noting two things: (i) We did not yet introduce a Hamiltonian. So far, we only studied how Bloch bands will transform under the space group symmetries. (ii) The way we constructed the Bloch bands they are defined as a representation of the space group. We call it an *elementary band representation* (EBR).
Example: For our choice of placing the orbitals $\overline{E}_{1g}$ and $\overline{E}_{2u}$ at $1a$, this process of induction is particularly trivial: There is only one Wyckoff position in the orbit and all point group symmetries act within the unit cell. Hence all $\boldsymbol{t}_{\alpha\beta} \equiv 0$ and $g^h_{\alpha\beta} \equiv h$. Therefore, the representations given in (9.2.7) and (9.2.9) define one-to-one the induced band representation.

9.2.3 Subducing a representation at special momenta

Theory: We have seen that in general the band representations connect two momenta. However, for every $\boldsymbol{k}$-point there exists a subgroup $G_{\boldsymbol{k}}$ of the full space group, under which $R\boldsymbol{k} = \boldsymbol{k}$ for all $R \in G_{\boldsymbol{k}}$ (up to a reciprocal lattice vector). The interesting, i.e., high-symmetry, points and lines in the Brillouin zone are those where this $G_{\boldsymbol{k}}$ does contain more than the trivial element.

$G_{\boldsymbol{k}}$ is called the *little group* of $\mathbf{k}$. We can see how the full band representation $[\rho_G^{\boldsymbol{k}}(h)]$ sub-duces irreps at these high-symmetry points.
Technically, the procedure is straight forward: Using the character table of the little group, we can reduce the full representation $[\rho_G^{\boldsymbol{k}}(h)]$ into the irreps $\sigma_i^{\boldsymbol{k}}$ of the little group via

$$[\rho_G^{\boldsymbol{k}}(h)] \downarrow G_{\boldsymbol{k}} = \bigoplus_i m_i \, \sigma_i^{\boldsymbol{k}}, \tag{9.2.19}$$

with

$$m_i = \frac{1}{n} \sum_h \chi_i^*(h) \chi_{[\rho_G^{\boldsymbol{k}}(h)]}(h), \tag{9.2.20}$$

where the sum is over all group elements h of the little group, $\chi_i(h)$ are the characters of the irreps $\sigma_i^{\boldsymbol{k}}$ and $\chi_{[\rho_G^{\boldsymbol{k}}(h)]}(h)$ is the character of the subduced representation. The parameter n is the order of the little group $G_{\boldsymbol{k}}$.
Example: Let us start with $\overline{E}_{1g}$. At the $\boldsymbol{\Gamma}$ point $\boldsymbol{k} = (0,0)$ we have the full group D_{4h}. For later reference, we go with the convention to use the second name of the irreps in Tab. 9.1 when we refer to the irreps of the little groups. In fact, we call the irreps by the name of the high-symmetry point supplemented by the number. E.g., $\overline{E}_{1g}$ at $\boldsymbol{\Gamma}$ is referred to as $\boldsymbol{\Gamma}_7$ and $\overline{E}_{2u}$ as $\boldsymbol{\Gamma}_8$.
If we now go out along the line $(k_x, 0)$ for $k_x \in [0, \pi]$ we reduce the little group to the double point group C_s with only a mirror as a non-trivial element. Using the character table in Tab. 9.1 and Eq. (9.2.20), we immediately find

$$m_{_2\overline{E}} = \frac{1}{4}(1 \times 2 + \mathrm{i} \times 0 + (-1) \times (-2) + (-\mathrm{i}) \times 0) = 1, \tag{9.2.21}$$

$$m_{_1\overline{E}} = \frac{1}{4}(1 \times 2 + (-\mathrm{i}) \times 0 + (-1) \times (-2) + \mathrm{i} \times 0) = 1. \tag{9.2.22}$$

$$\tag{9.2.23}$$

The same holds for $\overline{E}_{2u}$. This in principle means that the both irreps $\boldsymbol{\Gamma}_{7/8}$ split to $\overline{\boldsymbol{\Gamma}\boldsymbol{X}}_3$ and $\overline{\boldsymbol{\Gamma}\boldsymbol{X}}_4$ on the line from $\boldsymbol{\Gamma}$ to $\boldsymbol{X}$. If we also force time reversal symmetry $\mathcal{T}$, however, these two irreps have to come together as they form a conjugate pair (apparent through the complex characters for the mirror symmetry). For the lines $\overline{\boldsymbol{X}\boldsymbol{M}}$ and $\overline{\boldsymbol{M}\boldsymbol{\Gamma}}$ the same conclusion holds.
At $\boldsymbol{X}$ the little group is D_{2h} which again contains inversion. From this we can readily read off that the band representation induced by $\overline{E}_{1g}$ will subduce to $\boldsymbol{X}_5$ and $\overline{E}_{2u}$ to $\boldsymbol{X}_6$.
The $\boldsymbol{M}$ point has the same little group as $\boldsymbol{\Gamma}$ and hence we again find for $\overline{E}_{1g}$ the orbital $\boldsymbol{\Gamma}_7$ and for $\overline{E}_{2u}$ it is $\boldsymbol{\Gamma}_8$. Fig. 9.2(a) summarizes these considerations. Using the tools of the last few sections we constructed an explicit EBR and analyzed how the bands follow certain rules due to symmetry constraints. The following question presents itself: what kind of bands can arise in a given space group? This work has been done [1, 4] and we quickly introduce it in the next section before we analyze what happens when we place both $\overline{E}_{1g}$ *and* $\overline{E}_{2u}$ orbitals at $1a$.

9.2.4 A complete list of possible elementary band representations

Theory: The possible connections of the different irreps at different high-symmetry points in the Brillouin zone are highly restricted due to compatibility requirements. A complete tabulation of all EBRs has been achieved using spectral graph theory [1, 4]. The outcome of this work is available on the Bilbao Crystallographic Server under Topological Quantum Chemistry.
Example: Here we show in Tab 9.2 the results relevant for our example of spinful electrons in the planar version of $P4/mmm$. We see from this table that all induced representations from $1a$ and $1b$ positions follow the same pattern as the ones we considered in these notes. In particular, the compatibility requirements force these band representations to be *connected*: All irreps at the different high-symmetry points have to be linked by a dispersion line.

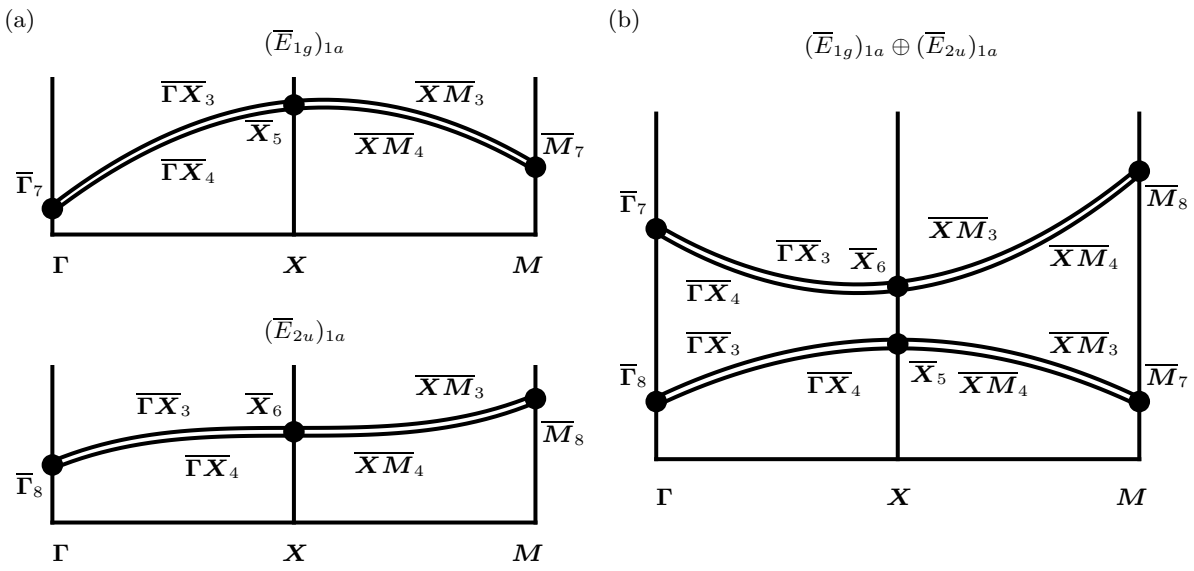

Figure 9.2: Band connectivities: (a) The bands induced by the orbitals $\overline{E}_{1g}$ and $\overline{E}_{2u}$ from Wyckoff position 1. Note that under time-reversal symmetry, the two irreps $\overline{\boldsymbol{AB}}_{3/4}$ are fused into a $2d$-irrep as they are conjugate to each other. (b) When the two EBRs of (a) overlap, one can connect the high-symmetry points in a way that gives rise to a stable topological insulator.

Wyckoff pos.	$1a$	$1a$	$1a$	$1a$	$1b$	$1b$	$1b$	$1b$	$2c$	$2c$
Site symm.	D_{4h}	D_{4h}	D_{4h}	D_{4h}	D_{4h}	D_{4h}	D_{4h}	D_{4h}	D_{2h}	D_{2h}
Orbital	$\overline{E}_{1g}$	$\overline{E}_{1u}$	$\overline{E}_{2g}$	$\overline{E}_{2u}$	$\overline{E}_{1g}$	$\overline{E}_{1u}$	$\overline{E}_{2g}$	$\overline{E}_{2u}$	$\overline{E}_g$	$\overline{E}_u$
Decomposable	x	x	x	x	x	x	x	x	✓	✓
$\boldsymbol{\Gamma}$	$\boldsymbol{\Gamma}_7$	$\boldsymbol{\Gamma}_9$	$\boldsymbol{\Gamma}_6$	$\boldsymbol{\Gamma}_8$	$\boldsymbol{\Gamma}_7$	$\boldsymbol{\Gamma}_9$	$\boldsymbol{\Gamma}_6$	$\boldsymbol{\Gamma}_8$	$\boldsymbol{\Gamma}_6 \oplus \boldsymbol{\Gamma}_7$	$\boldsymbol{\Gamma}_8 \oplus \boldsymbol{\Gamma}_9$
$\boldsymbol{M}$	$\boldsymbol{M}_7$	$\boldsymbol{M}_9$	$\boldsymbol{M}_6$	$\boldsymbol{M}_8$	$\boldsymbol{M}_6$	$\boldsymbol{M}_8$	$\boldsymbol{M}_7$	$\boldsymbol{M}_9$	$\boldsymbol{M}_8 \oplus \boldsymbol{M}_9$	$\boldsymbol{M}_6 \oplus \boldsymbol{M}_7$
$\boldsymbol{X}$	$\boldsymbol{X}_5$	$\boldsymbol{X}_6$	$\boldsymbol{X}_5$	$\boldsymbol{X}_6$	$\boldsymbol{X}_6$	$\boldsymbol{X}_5$	$\boldsymbol{X}_6$	$\boldsymbol{X}_5$	$\boldsymbol{X}_5 \oplus \boldsymbol{X}_6$	$\boldsymbol{X}_5 \oplus \boldsymbol{X}_6$

Table 9.2: Little-group irrep content of the EBRs for spinful orbitals in the space group $P4/mmm$.

The last two, which are induced from the Wyckoff position $2c$, with two sites in the orbit, are different. Here, the symmetry constraints allow for two sets of connected bands which are mutually disconnected. For the EBRs induced by $\overline{E}_g$ at $2c$ [which is often written as $(\overline{E}_g)_{2c}$] the options are

$$\begin{aligned} 1:&\ \boldsymbol{\Gamma}_6\text{—}\boldsymbol{M}_8\text{—}\boldsymbol{X}_5 \quad \text{and} \quad \boldsymbol{\Gamma}_7\text{—}\boldsymbol{M}_9\text{—}\boldsymbol{X}_6, \\ 2:&\ \boldsymbol{\Gamma}_6\text{—}\boldsymbol{M}_8\text{—}\boldsymbol{X}_6 \quad \text{and} \quad \boldsymbol{\Gamma}_7\text{—}\boldsymbol{M}_9\text{—}\boldsymbol{X}_5, \\ 3:&\ \boldsymbol{\Gamma}_7\text{—}\boldsymbol{M}_8\text{—}\boldsymbol{X}_5 \quad \text{and} \quad \boldsymbol{\Gamma}_6\text{—}\boldsymbol{M}_9\text{—}\boldsymbol{X}_6, \\ 4:&\ \boldsymbol{\Gamma}_7\text{—}\boldsymbol{M}_8\text{—}\boldsymbol{X}_6 \quad \text{and} \quad \boldsymbol{\Gamma}_6\text{—}\boldsymbol{M}_9\text{—}\boldsymbol{X}_5. \end{aligned} \tag{9.2.24}$$

For $(\overline{E}_u)_{2c}$ one finds

$$\begin{aligned} 1:&\ \boldsymbol{\Gamma}_8\text{—}\boldsymbol{M}_6\text{—}\boldsymbol{X}_5 \quad \text{and} \quad \boldsymbol{\Gamma}_9\text{—}\boldsymbol{M}_7\text{—}\boldsymbol{X}_6, \\ 2:&\ \boldsymbol{\Gamma}_8\text{—}\boldsymbol{M}_6\text{—}\boldsymbol{X}_6 \quad \text{and} \quad \boldsymbol{\Gamma}_9\text{—}\boldsymbol{M}_7\text{—}\boldsymbol{X}_5, \\ 3:&\ \boldsymbol{\Gamma}_9\text{—}\boldsymbol{M}_6\text{—}\boldsymbol{X}_5 \quad \text{and} \quad \boldsymbol{\Gamma}_8\text{—}\boldsymbol{M}_7\text{—}\boldsymbol{X}_6, \\ 4:&\ \boldsymbol{\Gamma}_9\text{—}\boldsymbol{M}_6\text{—}\boldsymbol{X}_6 \quad \text{and} \quad \boldsymbol{\Gamma}_8\text{—}\boldsymbol{M}_7\text{—}\boldsymbol{X}_5. \end{aligned} \tag{9.2.25}$$

We discuss the consequences of this table in the next section.

9.2.5 Stable and fragile topology

Theory: Table 9.2 together with Eq. (9.2.24) & (9.2.25) allows us to characterize bands in $P4/mmm$ according to their irrep content at high-symmetry points. There are three distinct scenarios:

Trivial bands

The irrep content of a given band structure can be written as a direct sum of the irreps in one of the EBRs in Tab. 9.2. This implies, that one can write a basis function of symmetric and localized orbitals, namely the ones from which these bands are induced.
For example, if we had a band structure with $\boldsymbol{\Gamma}_7 \oplus \boldsymbol{\Gamma}_7$, $\boldsymbol{M}_6 \oplus \boldsymbol{M}_7$, and $\boldsymbol{X}_5 \oplus \boldsymbol{X}_6$, we would immediately write

$$\left(\overline{E}_{1g}\right)_{1a} \oplus \left(\overline{E}_{1g}\right)_{1b}. \tag{9.2.26}$$

Stable topology

If, on the other hand, we need to make use of split bands [like the ones in Eq. (9.2.24) & (9.2.25)] to account for the irrep content of our bands, we cannot induce these bands from a set of symmetric localized orbitals: the definition of a topological system. We see one instance of such a stable topological set of bands in the example below.

Fragile topology

As a last option, there arises the possibility that one cannot reproduce the irrep content of the bands via a direct sum as in the trivial case above. However, as opposed to a split band, one might be able to collect the irreps of several EBRs in order to account for all irreps of the band under investigation. If in this process one accumulates too many degrees of freedom, one can maybe *subtract* the irreps of one or several other EBRs in order to account for the sought after types and multiplicities of irreps exactly. In this case one deals with *fragile topology*. Why is this topological: given that we need to add and subtract means that we cannot write a set of localized orbitals from which we can induce this set of bands. (There is no such thing as adding an atom with a minus sign). Why do we call it fragile: If one now adds a band induced by the orbital which appeared with a negative sign in the decomposition, we end up with a direct sum of elementary bands, and hence with a trivial system. One can summarize this by stating that a fragile topological system cannot be Wannierized, but becomes Wannierizable under the addition of a trivial band.

Example: As an example of how to use Tab. 9.2, we investigate what arises if we deal with a set of four bands induced by $(\overline{E}_{1g})_{1a}$ and $(\overline{E}_{2u})_{1a}$. In Fig. 9.2(b) we show what can happen if we bring the two EBRs close to each other. Remember that all lines are doubly degenerate because of the combination of the mirror symmetries with time reversal, i.e, all these double lines contain both mirror eigenvalues $\pm$i. As there are no further constraints, we can link up all irreps at $\boldsymbol{\Gamma}$, $\boldsymbol{M}$, and $\boldsymbol{X}$ at will.
The example shown in Fig. 9.2(b) can be understood has having exchanged the even and odd irreps (under inversion) at the $\boldsymbol{\Gamma}$ point, but not at the $\boldsymbol{X}$ or $\boldsymbol{M}$ points. In other words, we deal with the bands

$$\text{lower bands}: \boldsymbol{\Gamma}_7\text{—}\boldsymbol{M}_8\text{—}\boldsymbol{X}_6, \tag{9.2.27}$$

$$\text{upper bands}: \boldsymbol{\Gamma}_8\text{—}\boldsymbol{M}_7\text{—}\boldsymbol{X}_5. \tag{9.2.28}$$

When comparing to Tab. 9.2 we see that none of the EBRs fits this irrep content. However, when checking the split EBRs $(\overline{E}_g)_{2c}$ and $(\overline{E}_u)_{2c}$, we see that the two bands above and below the gap in Fig. 9.2(b) each arise from half an EBR! We deal with a stable topological system.

9.3 Finally: A Hamiltonian

So far, we have analyzed Bloch bands without making reference to a Hamiltonian. We got quite some mileage out of symmetry considerations alone! But now we would like to substantiate our findings on the stable topological system induced by $(\overline{E}_{1g})_{1a} \oplus (\overline{E}_{2u})_{1a}$. Let us remind ourselves of the time reversal invariant, doubled lattice Dirac Hamiltonian (4.3.2)

$$\mathcal{H} = \tau_0 \otimes \{[m - 2 + \cos(k_x) + \cos(k_y)]\sigma_z + \sin(k_y)\sigma_y\} + \sin(k_x)\tau_z \otimes \sigma_x. \tag{9.3.1}$$

For the purpose here, it is most convenient to transform to

$$\mathcal{H} \to U^\dagger \mathcal{H} U = \begin{pmatrix} \epsilon_0(\boldsymbol{k}) & 0 & l_+(\boldsymbol{k}) & 0 \\ 0 & \epsilon_0(\boldsymbol{k}) & 0 & -l_-(\boldsymbol{k}) \\ l_-(\boldsymbol{k}) & 0 & -\epsilon_0(\boldsymbol{k}) & 0 \\ 0 & -l_+(\boldsymbol{k}) & 0 & -\epsilon_0(\boldsymbol{k}) \end{pmatrix}, \quad \text{with} \quad U = \begin{pmatrix} 1 & 0 & 0 & 0 \\ 0 & 0 & 1 & 0 \\ 0 & 1 & 0 & 0 \\ 0 & 0 & 0 & 1 \end{pmatrix} \tag{9.3.2}$$

and

$$\epsilon_0(\boldsymbol{k}) = -2 + m + \cos(k_x) + \cos(k_y), \tag{9.3.3}$$

$$l_\pm = \sin(k_x) \pm \mathrm{i}\sin(k_y). \tag{9.3.4}$$

Written like this, it is apparent that the matrix elements $l_\pm(\boldsymbol{k})$ can raise (lower) the angular momentum quantum number by one. The Hamiltonian has the following symmetries

$$C_4^z: \quad (k_x, k_y) \to (k_y, -k_x) \qquad \rho(C_4^z) = \begin{pmatrix} e^{3\mathrm{i}\pi/4} & 0 & 0 & 0 \\ 0 & e^{-3\mathrm{i}\pi/4} & 0 & 0 \\ 0 & 0 & e^{\mathrm{i}\pi/4} & 0 \\ 0 & 0 & 0 & e^{-\mathrm{i}\pi/4} \end{pmatrix} \tag{9.3.5}$$

$$C_2^z: \quad (k_x, k_y) \to (-k_x, -k_y) \qquad \rho(C_2^z) = \begin{pmatrix} -\mathrm{i} & 0 & 0 & 0 \\ 0 & \mathrm{i} & 0 & 0 \\ 0 & 0 & -\mathrm{i} & 0 \\ 0 & 0 & 0 & \mathrm{i} \end{pmatrix} \tag{9.3.6}$$

$$C_2^y: \quad (k_x, k_y) \to (-k_x, k_y) \qquad \rho(C_2^y) = \begin{pmatrix} 0 & \mathrm{i} & 0 & 0 \\ \mathrm{i} & 0 & 0 & 0 \\ 0 & 0 & 0 & \mathrm{i} \\ 0 & 0 & \mathrm{i} & 0 \end{pmatrix} \tag{9.3.7}$$

$$I: \quad (k_x, k_y) \to (-k_x, -k_y) \qquad \rho(I) = \begin{pmatrix} -1 & 0 & 0 & \\ 0 & -1 & 0 & 0 \\ 0 & 0 & 1 & 0 \\ 0 & 0 & 0 & 1 \end{pmatrix} \tag{9.3.8}$$

Comparing this to the representations in $\overline{E}_{1g}$ (9.2.7) and $\overline{E}_{2u}$ (9.2.9) we immediately see that we deal with $P4/mmm$ and that the first two orbitals correspond to $\overline{E}_{2u}$, while the second two belong to $\overline{E}_{1g}$.

To determine the irrep content at the high-symmetry momenta $\boldsymbol{\Gamma}$, $\boldsymbol{X}$, and $\boldsymbol{M}$ we only need to look at the eigenvalues of $\rho(I)$, as inversion determines the difference between the involved irreps $\boldsymbol{\Gamma}_{7/8}$, $\boldsymbol{M}_{7/8}$, and $\boldsymbol{X}_{5/6}$, respectively. At the high-symmetry points, the Hamiltonian reads

$$\mathcal{H}(\boldsymbol{\Gamma}) = \mathrm{diag}(m, m, -m, -m), \tag{9.3.9}$$

$$\mathcal{H}(\boldsymbol{X}) = \mathrm{diag}(-2 + m, -2 + m, 2 - m, 2 - m), \tag{9.3.10}$$

$$\mathcal{H}(\boldsymbol{M}) = \mathrm{diag}(-4 + m, -4 + m, 4 - m, 4 - m). \tag{9.3.11}$$

$m < 0$: The first two states are odd under inversion. For $m < 0$, they form the lower two bands at all high-symmetry momenta. Therefore, we realize

$$\text{lower}: \quad (\overline{E}_{2u})_{1a} \qquad \text{upper}: \quad (\overline{E}_{1g})_{1a}. \tag{9.3.12}$$

$0 < m < 2$: Now, the inversion eigenvalue switches at $\boldsymbol{\Gamma}$. Hence we realize $\boldsymbol{\Gamma}_7$—$\boldsymbol{M}_8$—$\boldsymbol{X}_6$ in the lower and $\boldsymbol{\Gamma}_8$—$\boldsymbol{M}_7$—$\boldsymbol{X}_5$ in the upper band. We can write the bands as

$$\text{lower}: \quad \frac{1}{2}(\overline{E}_{g})_{2c} \qquad \text{upper}: \quad \frac{1}{2}(\overline{E}_{u})_{2c}, \tag{9.3.13}$$

from which we read off that we deal with a stable topological insulator.
$2 < m < 4$: At $m = 2$, the gap closes at $\boldsymbol{X}$ and now also at $\boldsymbol{X}$ the lower bands are even under inversion. Hence we realize $\boldsymbol{\Gamma}_7$—$\boldsymbol{M}_8$—$\boldsymbol{X}_5$ in the lower and $\boldsymbol{\Gamma}_8$—$\boldsymbol{M}_7$—$\boldsymbol{X}_6$ in the upper band. While different split versions of the EBRs induced at $2c$ are realized, the bands can still be written as

$$\text{lower}: \quad \frac{1}{2}(\overline{E}_{g})_{2c} \qquad \text{upper}: \quad \frac{1}{2}(\overline{E}_{u})_{2c}. \tag{9.3.14}$$

$m > 4$: For $m > 4$, finally, all irreps of the lower bands are even under inversion and we have

$$\text{lower}: \quad (\overline{E}_{1g})_{1a} \qquad \text{upper}: \quad (\overline{E}_{2u})_{1a}. \tag{9.3.15}$$

References

1. Bradlyn, B. *et al.* "Topological quantum chemistry". *Nature* **537,** 298. https://dx.doi.org/10.1038/nature23268 (2017).
2. Robredo, I., Bernevig, B. A. & Mañes, J. L. in (eds Bercioux, D., Cayssol, J., Vergniory, M. G. & Calvo, M.) 1 (Springer Nature Switzerland, 2018). https://doi.org/10.1007/978-3-319-76388-0_1.
3. Kohn, W. "Analytic properties of bloch waves and wannier functions". *Phys. Rev.* **115,** 809. http://link.aps.org/abstract/PR/v115/p809 (1959).
4. Bradlyn, B. *et al.* "Band connectivity for topological quantum chemistry: Band structures as a graph theory problem". *Phys. Rev. B* **97,** 035138. https://doi.org/10.1103/PhysRevB.97.035138 (2018).